AMERICAN SOCIETY FOR MICROBIOLOGY | Microbiology Spectrum

RESEARCH ARTICLE

Diaphorin, a Polyketide Produced by a Bacterial Symbiont of the Asian Citrus Psyllid, Inhibits the Growth and Cell Division of *Bacillus subtilis* but Promotes the Growth and Metabolic Activity of *Escherichia coli*

Nozomu Tanabe,[a] Rena Takasu,[a] Yuu Hirose,[a] Yasuhiro Kamei,[b] Maki Kondo,[b] Atsushi Nakabachi[a,c]

[a]Department of Environmental and Life Sciences, Toyohashi University of Technology, Toyohashi, Aichi, Japan
[b]Optics and Imaging Facility, Trans-Scale Biology Center, National Institute for Basic Biology, Okazaki, Aichi, Japan
[c]Electronics-Inspired Interdisciplinary Research Institute (EIIRIS), Toyohashi University of Technology, Toyohashi, Aichi, Japan

ABSTRACT Diaphorin is a polyketide produced by "*Candidatus* Profftella armatura" (*Gammaproteobacteria*: *Burkholderiales*), an obligate symbiont of a notorious agricultural pest, the Asian citrus psyllid *Diaphorina citri* (Hemiptera: Psyllidae). Diaphorin belongs to the pederin family of bioactive agents found in various host-symbiont systems, including beetles, lichens, and sponges, harboring phylogenetically diverse bacterial producers. Previous studies showed that diaphorin, which is present in *D. citri* at concentrations of 2 to 20 mM, has inhibitory effects on various eukaryotes, including the natural enemies of *D. citri*. However, little is known about its effects on prokaryotic organisms. To address this issue, the present study assessed the biological activities of diaphorin on two model prokaryotes, *Escherichia coli* (*Gammaproteobacteria*: *Enterobacterales*) and *Bacillus subtilis* (*Firmicutes*: *Bacilli*). Their growth and morphological features were analyzed using spectrophotometry, optical microscopy followed by image analysis, and transmission electron microscopy. The metabolic activity of *E. coli* was further assessed using the β-galactosidase assay. The results revealed that physiological concentrations of diaphorin inhibit the growth and cell division of *B. subtilis* but promote the growth and metabolic activity of *E. coli*. This finding implies that diaphorin functions as a defensive agent of the holobiont (host plus symbionts) against some bacterial lineages but is metabolically beneficial for others, which potentially include obligate symbionts of *D. citri*.

IMPORTANCE Certain secondary metabolites, including antibiotics, evolve to mediate interactions among organisms. These molecules have distinct spectra for microorganisms and are often more effective against Gram-positive bacteria than Gram-negative ones. However, it is rare that a single molecule has completely opposite activities on distinct bacterial lineages. The present study revealed that a secondary metabolite synthesized by an organelle-like bacterial symbiont of psyllids inhibits the growth of Gram-positive *Bacillus subtilis* but promotes the growth of Gram-negative *Escherichia coli*. This finding not only provides insights into the evolution of microbiomes in animal hosts but also may potentially be exploited to promote the effectiveness of industrial material production by microorganisms.

KEYWORDS "*Candidatus* Profftella armatura," *Diaphorina citri*, pederin family, secondary metabolite, symbiosis

Microorganisms produce diverse secondary metabolites that mediate competition, communication, and other interactions with surrounding organisms (1–4). Such molecules have various biological activities, some of which facilitate symbiosis between microorganisms and animal hosts (5–8).

Editor Daifeng Cheng, South China Agricultural University

Address correspondence to Atsushi Nakabachi, nakabachi.atsushi.ro@tut.jp.

The authors declare no conflict of interest.

Received 13 May 2022
Accepted 8 July 2022
Published 27 July 2022

The Asian citrus psyllid *Diaphorina citri* Kuwayama (Hemiptera: Sternorrhyncha: Psylloidea: Psyllidae) is an important agricultural pest that transmits "*Candidatus* Liberibacter spp." (*Alphaproteobacteria*: *Rhizobiales*), the causative agents of a devastating citrus disease known as huanglongbing (HLB) or greening disease (9–12). Because HLB is currently incurable, controlling *D. citri* is presently the most crucial part of HLB management (9, 12). Although the application of chemical insecticides is currently the primary option for controlling *D. citri*, more sustainable strategies, including its biological control, are warranted (9, 13–15), partly due to the global increase in the resistance of *D. citri* to various pesticides (16–18).

The *D. citri* hemocoel contains a symbiotic organ called the bacteriome (19, 20), which harbors two distinct obligate mutualists, "*Candidatus* Carsonella ruddii" (*Gammaproteobacteria*: *Oceanospirillales*) and "*Candidatus* Profftella armatura" (*Gammaproteobacteria*: *Burkholderiales*) (21, 22). "*Candidatus* Carsonella" is a typical nutritional symbiont, providing its host with essential amino acids that are scarce in the phloem sap diet (21, 23, 24). In contrast, "*Candidatus* Profftella" appears to be an organelle-like defensive symbiont, producing toxins that protect the holobiont (host plus symbionts) from natural enemies (21, 25). "*Candidatus* Profftella" has a very small genome, at 460 kb, a large part of which is devoted to a gene set to synthesize a polyketide, diaphorin (21). Diaphorin is an analog of pederin (21), a defensive polyketide that accumulates in the body fluid of *Paederus* rove beetles (Coleoptera: Staphylinidae) to deter predators (26–28). Previous studies have demonstrated that diaphorin, which is present at a concentration as high as 2 to 20 mM in *D. citri*, depending on its life stage (29), has inhibitory effects on various eukaryotic organisms, suggesting that it helps protect *D. citri* from eukaryotic predators, parasitoids, parasites, and pathogens (21, 25, 30). Recent studies have revealed that "*Candidatus* Profftella" and its gene clusters for synthesizing diaphorin are conserved in relatives of *D. citri*, suggesting the physiological and ecological importance of diaphorin for the host insect (31, 32). However, little is known about the effects of diaphorin on prokaryotic organisms, which potentially affect the internal and external microbiomes of insects.

As a first step to address this issue, this study assessed the biological activities of diaphorin on *Escherichia coli* (*Gammaproteobacteria*: *Enterobacterales*) and *Bacillus subtilis* (*Firmicutes*: *Bacilli*), which are model organisms for Gram-negative and Gram-positive bacteria, respectively. The growth and morphological features of these bacteria were analyzed using spectrophotometry, optical microscopy followed by image analysis, and transmission electron microscopy (TEM). The metabolic activity of *E. coli* was further assessed using the β-galactosidase assay.

RESULTS

Diaphorin promoted the growth of *E. coli*. To assess the effects of diaphorin on *E. coli*, *E. coli* strain JM109 cells were cultured in an LB medium with 100 μg/mL of ampicillin supplemented with 0, 5, 50, or 500 μM or 5 mM diaphorin (Fig. 1A). Four temporally independent experiments were performed, each consisting of three independent cultures in three independent tubes per treatment, giving 12 independent cultures ($n = 12$) per treatment. From after 6 h until the end of incubation (24 h), the change in optical density at 600 nm (ΔOD_{600}) of *E. coli* cultivated in a medium containing 5 mM diaphorin was significantly higher than that of *E. coli* cultured in a medium without diaphorin ($P < 0.05$, Dunnett's test [Fig. 1A]). The ratio of the ΔOD_{600} of the 5 mM diaphorin group to the ΔOD_{600} of the control group reached the maximum of 1.40 at 7 h, corresponding to the logarithmic growth phase. The medium containing 5 mM diaphorin but without inoculation of *E. coli* showed no increase in OD_{600}, indicating that diaphorin does not directly affect OD_{600} in the culture medium. The ΔOD_{600} of *E. coli* cultured in a medium containing 5, 50, and 500 μM diaphorin showed no significant difference from that of *E. coli* cultured in a medium without diaphorin ($P > 0.05$, Dunnett's test [Fig. 1A]). High-throughput amplicon sequencing of the 16S rRNA gene showed that 99.992% (277,249 reads of the 277,271 total reads) and 99.995% (228,262 reads of the 228,274 total reads) of the reads derived from cultures treated with 0 and

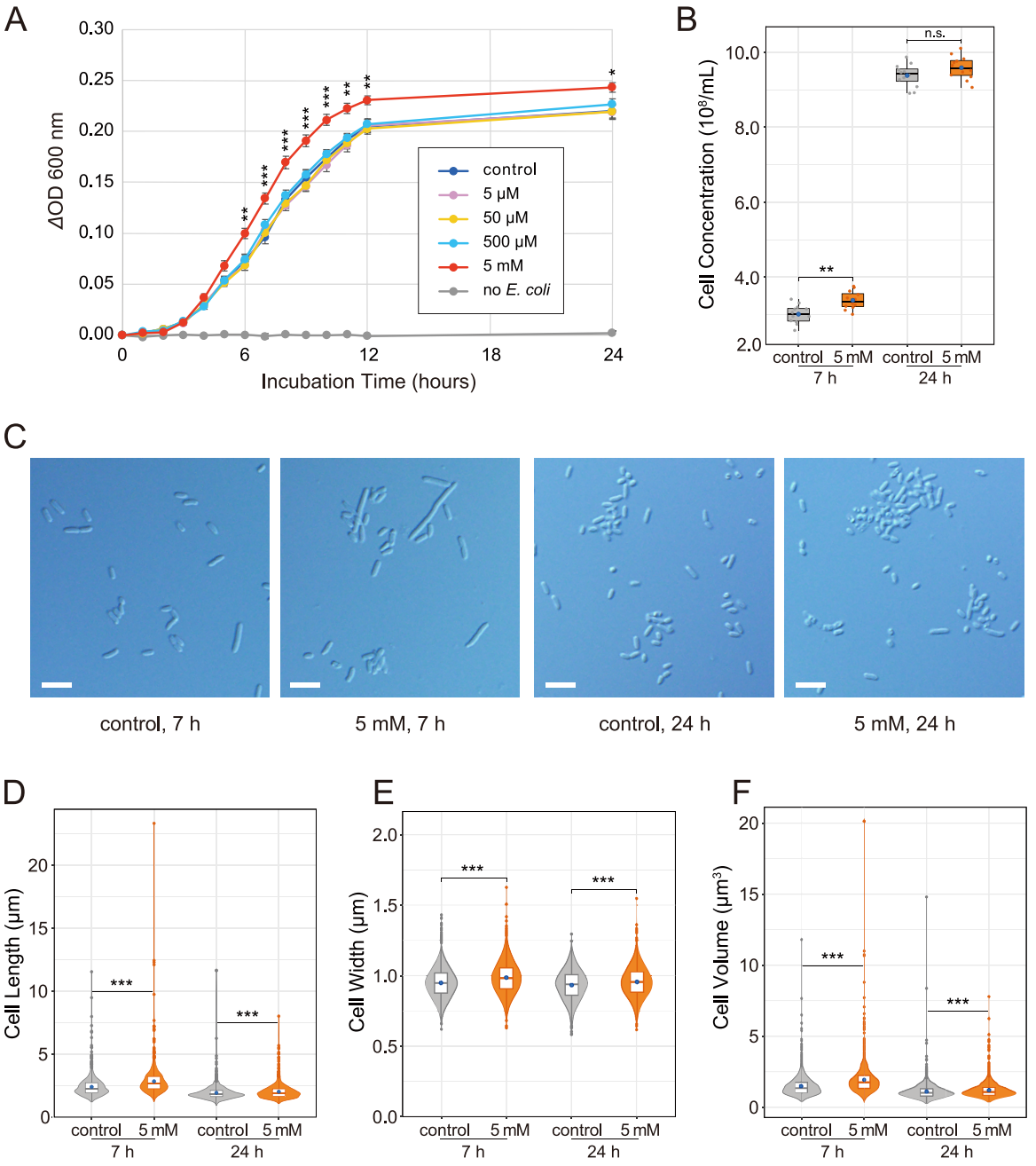

FIG 1 Evaluation of the biological activity of diaphorin on the growth of *E. coli*. (A) Growth dynamics of *E. coli* cultured in a medium containing 0, 5, 50, and 500 μM and 5 mM diaphorin. The change of OD_{600} (ΔOD_{600}) obtained by subtracting the value of each culture in each tube at time zero is presented. Each data point represents the mean of 12 independent cultures (n = 12). Error bars represent standard errors (SEs). Asterisks indicate statistically significant differences (*, $P < 0.05$; **, $P < 0.01$; ***, $P < 0.001$; Dunnett's test). To show the lack of direct effects of diaphorin on ΔOD_{600}, data for a medium containing 5 mM diaphorin but without inoculation of *E. coli* are also presented (n = 3). (B) Concentrations of *E. coli* cells cultured for 7 h (left) and 24 h (right). Jitter plots of all data points (n = 12) and box plots (gray, control; orange, 5 mM diaphorin) showing their distributions (median, quartiles, minimum, and maximum) are presented. Each data point is an average count obtained from 10 independent counting areas in a bacterial counter. Blue dots represent their means. Asterisks indicate the statistically significant difference (**, $P < 0.01$; Welch's t test). n.s., not significant. (C) DIC images of *E. coli* cultured in a medium containing 0 or 5 mM diaphorin for 7 or 24 h. Bars, 5 μm. (D) Violin plots (kernel density estimation) overlaid with box plots (median, quartiles, minimum, and maximum) and small dots (outliers) show distributions of cell lengths of *E. coli* cultured in a medium containing 0 mM (gray; n = 1,200) or 5 mM (orange; n = 1,200) diaphorin for 7 h (left) or 24 h (right). Blue dots represent the means. Asterisks indicate statistically significant differences (***, $P < 0.001$; Steel-Dwass test). (E) Distributions of cell widths of *E. coli* cultured in a medium containing 0 mM (gray; n = 1,200) or 5 mM (orange, n = 1,200) diaphorin for 7 h (left) or 24 h (right). Symbols are the same as in panel D. (F) Distributions of cell volumes of *E. coli* cultured in a medium containing 0 mM (gray; n = 1,200) or 5 mM (orange; n = 1,200) diaphorin for 7 h (left) or 24 h (right). Symbols are the same as in panel D.

5 mM diaphorin, respectively, corresponded to *E. coli* sequences, indicating that contamination was negligible (see Table S1 in the supplemental material).

To further examine the status of *E. coli* in these cultures, the cell concentration (numbers per milliliter) of cultures with and without supplementation of 5 mM diaphorin was assessed (Fig. 1B). Sampling time points were at 7 and 24 h, corresponding to the logarithmic and the stationary phases, respectively (Fig. 1A). Differential interference contrast (DIC) images of *E. coli* at these time points are shown in Fig. 1C. Aliquots of 12 cultures from each treatment were put into a bacterial counter, and 10 independent counting areas were used to calculate the mean concentration for each culture (Fig. 1B). At 7 h of incubation, the cell concentration of cultures treated with 5 mM diaphorin was (3.38 $\pm$ 0.24) $\times$ 10^8/mL (mean $\pm$ standard deviation [SD]; n = 12), which was slightly (12.3%) but significantly higher than that of control cultures, (3.01 $\pm$ 0.25) $\times$ 10^8/mL (n = 12; $P < 0.01$, Welch's t test [Fig. 1B]). At 24 h of incubation, cell concentrations were not significantly different between cultures treated with 5 mM diaphorin ([9.58 $\pm$ 0.31] $\times$ 10^8/mL [n = 12]) and control cultures ([9.38 $\pm$ 0.30] $\times$ 10^8/mL [n = 12]; $P > 0.05$, Welch's t test).

As these results showed that the increased cell concentration is not fully accountable for the observed effects of diaphorin on ΔOD_{600} of *E. coli* cultures, the morphology of *E. coli* in these cultures was subsequently assessed (Fig. 1D to F). At 7 h of incubation, the length of cells treated with 5 mM diaphorin was 2.84 $\pm$ 1.18 μm (mean $\pm$ SD; n = 1,200), which was significantly larger than that of control cells, 2.41 $\pm$ 0.77 μm (n = 1,200; $P < 0.001$, Steel-Dwass test [Fig. 1D]). At 24 h of incubation, the length of cells treated with 5 mM diaphorin was 2.02 $\pm$ 0.56 μm (n = 1,200), which was also significantly larger than that of control cells, 1.93 $\pm$ 0.60 μm (n = 1,200; $P < 0.001$, Steel-Dwass test [Fig. 1D]). Similarly, at 7 h of incubation, the width of cells treated with 5 mM diaphorin was 0.99 $\pm$ 0.12 μm (n = 1,200), which was significantly larger than that of control cells, 0.95 $\pm$ 0.11 μm (n = 1,200; $P < 0.001$, Steel-Dwass test [Fig. 1E]). At 24 h of incubation, the width of cells treated with 5 mM diaphorin was 0.96 $\pm$ 0.11 μm (n = 1,200), which was also significantly larger than that of control cells, 0.93 $\pm$ 0.11 μm (n = 1,200; $P < 0.001$, Steel-Dwass test [Fig. 1E]). Regarding cell volumes calculated from observed lengths and widths, the value of cells cultured with 5 mM diaphorin for 7 h was 1.97 $\pm$ 1.10 μm^3 (n = 1,200), which was significantly larger (29.4%) than that of control cells, 1.52 $\pm$ 0.76 μm^3 (n = 1,200; $P < 0.001$, Steel-Dwass test [Fig. 1F]). The volume of cells cultured with 5 mM diaphorin for 24 h was 1.26 $\pm$ 0.61 μm^3 (n = 1,200), which was slightly (9.9%) but significantly larger than that of control cells, 1.14 $\pm$ 0.63 μm^3 (n = 1,200; $P < 0.001$, Steel-Dwass test [Fig. 1F]). These results demonstrated that diaphorin, at physiological concentrations in *D. citri*, increases the concentration and cell size of *E. coli*, suggesting that diaphorin promotes the growth of *E. coli*.

Diaphorin activated the metabolism of *E. coli*. To gain some insights into the metabolic activity of *E. coli*, the β-galactosidase assay was performed using *E. coli* treated or not with 5 mM diaphorin (Fig. 2; see Table S2 for values of each parameter). At the logarithmic growth phase, *E. coli* cells were incubated with 1 mM isopropyl β-D-1-thiogalactopyranoside (IPTG) for 3 h to induce the expression of β-galactosidase. The Miller unit value (ΔOD_{420} per minute per milliliter per OD_{600}) of *E. coli* treated with 5 mM diaphorin was 524 $\pm$ 52 (mean $\pm$ SD; n = 20), which was slightly (6.9%) but significantly larger than that of the control, 490 $\pm$ 54 (n = 20; $P < 0.05$, Welch's t test [Fig. 2A]). This result suggested that diaphorin activates the metabolic activity of *E. coli*. The Miller unit is based on a formula including division by OD_{600}, intending to calibrate the enzymatic activity with cell density or biomass of the sample (33). When this calibration was omitted to show the enzymatic activity per culture volume, the β-galactosidase activity (ΔOD_{420} per minute per milliliter) of *E. coli* treated with 5 mM diaphorin was calculated to be 80.4 $\pm$ 16.9 (n = 20), which was significantly and remarkably (52.0%) larger than that of control *E. coli*, 52.9 $\pm$ 7.8 (n = 20; $P < 0.001$, Welch's t test [Fig. 2B]). This result suggested that diaphorin notably activates the metabolic activity of *E. coli* per culture volume.

Electron microscopy showed the normality of *E. coli* treated with diaphorin. To assess the ultrastructure of *E. coli* treated with diaphorin, transmission electron

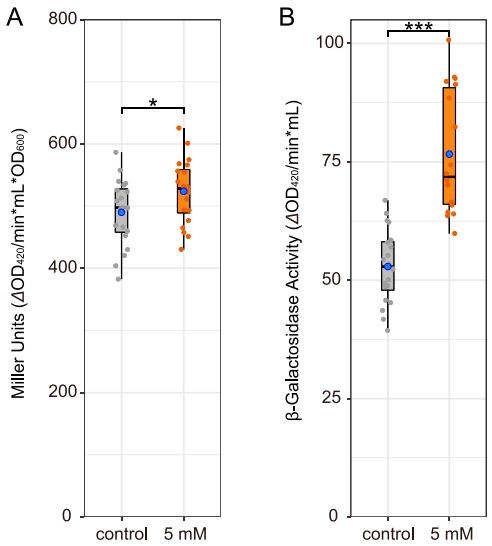

FIG 2 β-Galactosidase activity in *E. coli* cultures treated with and without diaphorin. Jitter plots of all data points ($n = 20$) and box plots (gray, control; orange, 5 mM diaphorin) showing their distributions (median, quartiles, minimum, and maximum) are presented. Blue dots represent the means. (A) β-Galactosidase activity in the form of Miller unit, $1{,}000 \times [(OD_{420} - 1.75 \times OD_{550})/(t \times v \times OD_{600})]$, where t is time of the enzymatic reaction (minutes) and v is volume of culture used in the assay (milliliters), showing the activity relative to the cell biomass. The asterisk indicates the statistically significant difference (*, $P < 0.05$; Welch's t test). (B) β-Galactosidase activity without calibration with OD_{600}, $1{,}000 \times [(OD_{420} - 1.75 \times OD_{550})/(t \times v)]$, showing the activity relative to the culture volume. Asterisks indicate the statistically significant difference (***, $P < 0.001$; Welch's t test).

microscopy (TEM) was performed using *E. coli* cultured for 7 h in a medium containing 0 mM (Fig. 3A to D) or 5 mM (Fig. 3E to H) diaphorin. Results showed no conspicuous difference in the ultrastructure between control and diaphorin-treated *E. coli*, suggesting that *E. coli* treated with diaphorin is normal.

Diaphorin inhibited the growth of *B. subtilis*. To assess the effects of diaphorin on *B. subtilis*, *B. subtilis* strain ISW1214 cells were cultured in an L broth medium containing 20 μg/mL of tetracycline supplemented with 0, 5, 50, or 500 μM or 5 mM diaphorin (Fig. 4A). Four temporally independent experiments were performed, each consisting of three independent cultures in three independent tubes per treatment, giving 12 independent cultures ($n = 12$) per treatment. From after 3 h until the end of incubation (24 h), the ΔOD_{600} of *B. subtilis* cultured in a medium containing 5 mM diaphorin was significantly lower than that of *B. subtilis* cultured in a medium without diaphorin ($P < 0.001$, Dunnett's test). The ΔOD_{600} of *B. subtilis* treated with 500 μM diaphorin was also significantly lower than that of control *B. subtilis* after incubation for 5 to 24 h ($P < 0.001$, Dunnett's test). The ΔOD_{600} of *B. subtilis* cultured in a medium containing 5 and 50 μM diaphorin showed no significant difference from that of *B. subtilis* cultured in a medium without diaphorin ($P > 0.05$, Dunnett's test). Two-way analysis of variance (ANOVA) revealed significant dosage effects of diaphorin ($F_{4,\ 770} = 423.3$; $P < 0.001$). The results of Tukey's multiple-comparison test are summarized in Table S3. The medium containing 5 mM diaphorin but without inoculation of *B. subtilis* showed no increase in OD_{600} (Fig. 4A), indicating that diaphorin does not directly affect OD_{600} in the culture medium. High-throughput amplicon sequencing of the 16S rRNA gene showed that 100% of the reads (258,404 and 218,754 reads from control cultures and cultures treated with 5 mM diaphorin, respectively) corresponded to *B. subtilis* sequences, indicating that there was essentially no contamination (Table S4). The growth dynamics shown in this study demonstrated that diaphorin, at physiological concentrations in *D. citri*, inhibits the growth of *B. subtilis*, contrasting the case with *E. coli*.

To further examine the status of *B. subtilis* in these cultures, the cell concentration (numbers per milliliter) of cultures with and without supplementation of 5 mM diaphorin was assessed (Fig. 4B). Sampling time points were 12 and 24 h. DIC images of *B. subtilis* at these time points are shown in Fig. 4C. Aliquots of 12 cultures from each

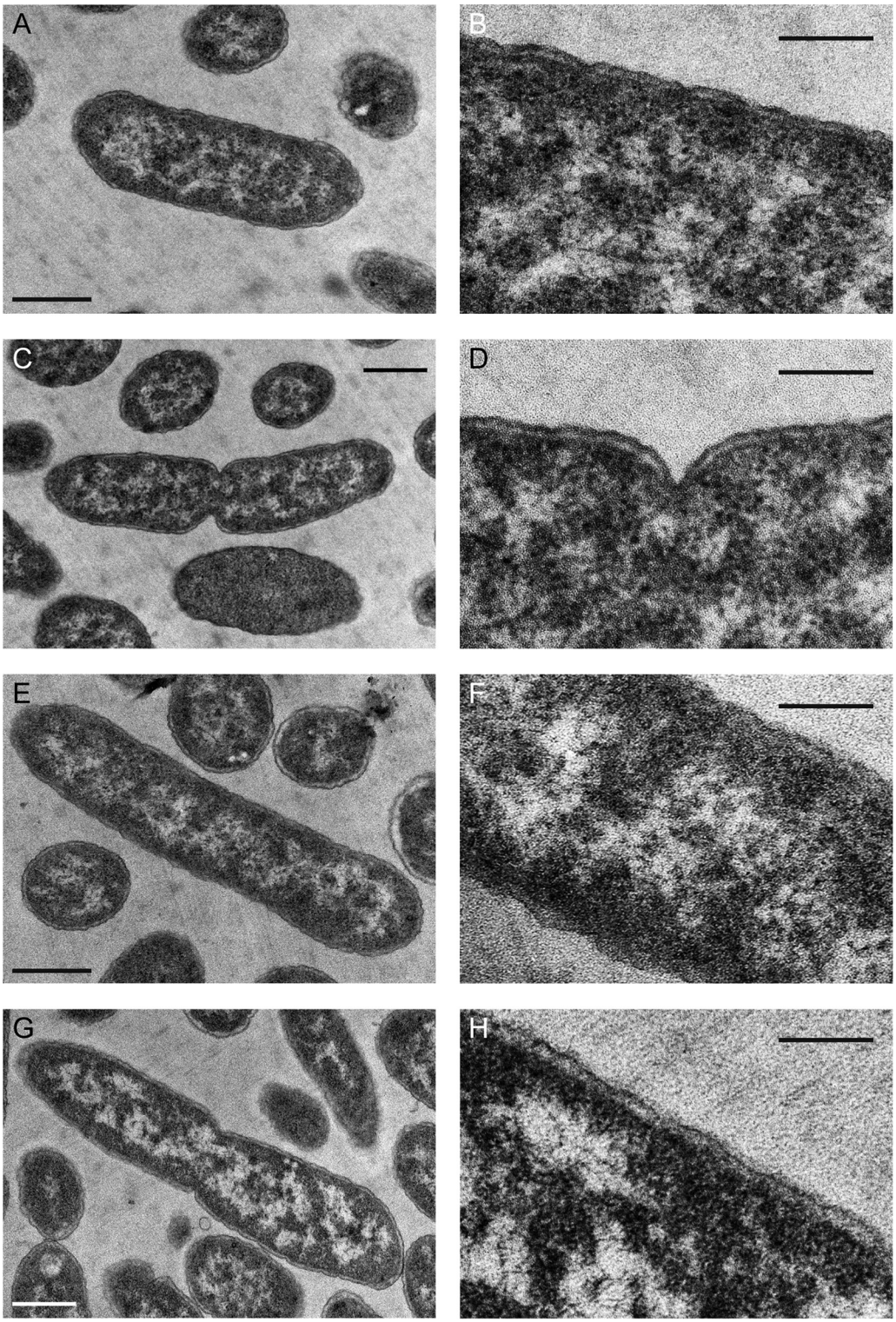

FIG 3 TEM of *E. coli* cultured for 7 h in a medium containing 0 mM (A to D) or 5 mM (E to H) diaphorin. Panels B, D, F, and H (bars, 200 nm) are magnified images of panels A, C, E, and G (bars, 500 nm), respectively. No conspicuous difference was observed in the ultrastructures between control and diaphorin-treated *E. coli*.

treatment were put into a bacterial counter, and 10 independent counting areas were used to calculate the mean concentration for each culture. At 12 h of incubation, the cell concentration of cultures treated with 5 mM diaphorin was $(0.03 \pm 0.00) \times 10^8$/mL (mean $\pm$ SD; $n = 12$), which was significantly lower than that of control cultures,

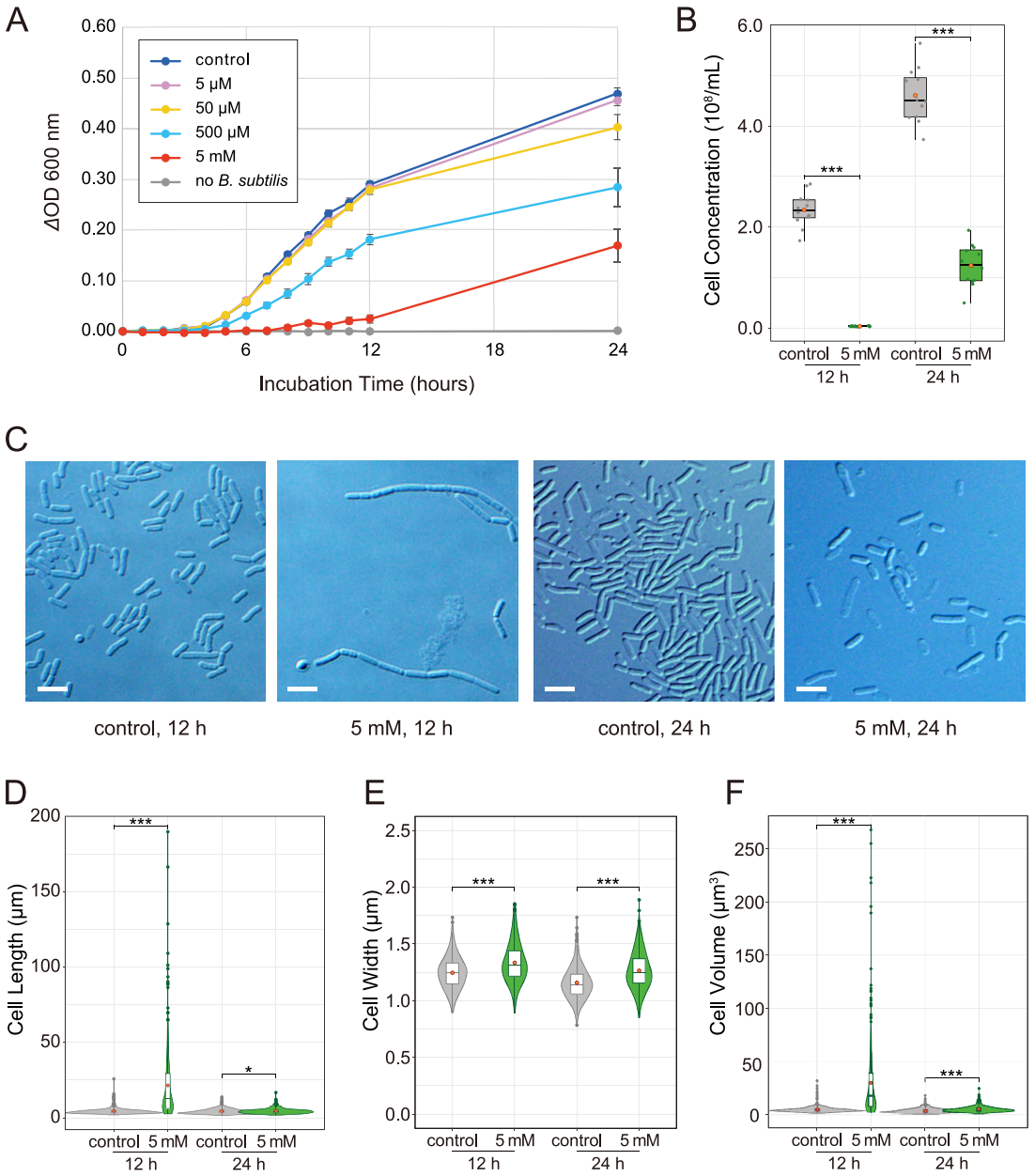

FIG 4 Evaluation of the biological activity of diaphorin on the growth of *B. subtilis*. (A) Growth dynamics of *B. subtilis* cultured in a medium containing 0, 5, 50, and 500 μM and 5 mM diaphorin. The change of OD_{600} (ΔOD_{600}) obtained by subtracting the value of each culture in each tube at time zero is presented. Each data point represents the mean of 12 cultures (n = 12). Error bars represent SEs. To show the lack of direct effects of diaphorin on ΔOD_{600}, data for a medium containing 5 mM diaphorin but without inoculation of *B. subtilis* are also presented (n = 3). (B) Concentrations of *B. subtilis* cells cultured for 12 h (left) and 24 h (right). Jitter plots of all data points (n = 12) and box plots (gray, control; green, 5 mM diaphorin) showing their distributions (median, quartiles, minimum, maximum) are presented. Each data point is an average count obtained from 10 independent counting areas in a bacterial counter. Orange dots represent their means. Asterisks indicate statistically significant differences (***, $P < 0.001$; Welch's t test). (C) DIC images of *B. subtilis* cultured in a medium containing 0 or 5 mM diaphorin for 12 or 24 h. Bars, 5 μm. (D) Violin plots (kernel density estimation) overlaid with box plots (median, quartiles, minimum, maximum) and small dots (outliers) show distributions of cell length of *B. subtilis* cultured in a medium containing 0 mM (gray; n = 400) or 5 mM (green; n = 400) diaphorin for 12 h (left) or 24 h (right). Orange dots represent the means. Asterisks indicate statistically significant differences (*, $P < 0.05$; ***, $P < 0.001$; Steel-Dwass test). (E) Distributions of cell widths of *B. subtilis* cultured in a medium containing 0 mM (gray; n = 400) or 5 mM (green; n = 400) diaphorin for 12 h (left) or 24 h (right). Symbols are the same as in panel D. (F) Distributions of cell volumes of *B. subtilis* cultured in a medium containing 0 mM (gray; n = 400) or 5 mM (green; n = 400) diaphorin for 12 h (left) or 24 h (right). Symbols are the same as in panel D.

(2.34 ± 0.33) × 10^8/mL (n = 12; $P < 0.001$, Welch's t test [Fig. 4B]). At 24 h of incubation, the cell concentration of cultures treated with 5 mM diaphorin was (1.24 ± 0.41) × 10^8/mL (n = 12), which was also significantly lower than that of control cultures, (4.60 ± 0.54) × 10^8/mL (n = 12; $P < 0.001$, Welch's t test [Fig. 4B]).

Subsequently, the morphology of *B. subtilis* cells in these cultures was assessed (Fig. 4D to F). At 12 h of incubation, cells treated with 5 mM diaphorin were as long as 21.54 ± 22.82 μm (mean ± SD; n = 400), which was significantly larger than control cells, 4.56 ± 2.27 μm (n = 400; $P < 0.001$, Steel-Dwass test [Fig. 4D]). In contrast, the length of the Hoechst-stained nucleoid area of *B. subtilis* cultured with 5 mM diaphorin for 12 h was 1.99 ± 0.59 μm (n = 400), which was significantly smaller than that of control cells, 2.51 ± 0.92 μm (n = 400; $P < 0.001$, Brunner-Munzel test [Fig. S1]), suggesting that diaphorin inhibits not only the growth but also the cleavage of *B. subtilis* cells. The length of cells cultured with 5 mM diaphorin for 24 h was 4.58 ± 1.82 μm (n = 400), which remained significantly larger than that of control cells, 4.30 ± 1.77 μm (n = 400; $P < 0.05$, Steel-Dwass test [Fig. 4D]). Whereas the length of control cells was not significantly different between time points 12 and 24 h ($P > 0.05$, Steel-Dwass test), the length of cells treated with 5 mM diaphorin was significantly reduced at 24 h ($P < 0.001$, Steel-Dwass test). Regarding cell width, the value for *B. subtilis* cultured with 5 mM diaphorin for 12 h was 1.33 ± 0.17 μm (n = 400), which was again significantly larger than that of control cells, 1.24 ± 0.14 μm (n = 400; $P < 0.001$, Steel-Dwass test [Fig. 4E]). At 24 h of incubation, the width of cells treated with 5 mM diaphorin was 1.26 ± 0.16 μm (n = 400), which was also significantly larger than that of control cells, 1.16 ± 0.14 μm (n = 400) ($P < 0.001$, Steel-Dwass test). Diaphorin-treated and control cells showed significantly reduced width from 12 to 24 h ($P < 0.001$, Steel-Dwass test [Fig. 4E]). As for the cell volume, that for *B. subtilis* treated with 5 mM diaphorin for 12 h was as high as 30.50 ± 35.51 μm^3 (n = 400), which was significantly larger than that of control cells, 5.15 ± 3.29 μm^3 (n = 400; $P < 0.001$, Steel-Dwass test [Fig. 4F]). At 24 h of incubation, the volume of cells treated with 5 mM diaphorin was 5.40 ± 3.02 μm^3 (n = 400), which was also significantly larger than that of control cells, 4.26 ± 2.38 μm^3 (n = 400; $P < 0.001$, Steel-Dwass test). Diaphorin-treated and control cells showed significantly reduced volume from 12 to 24 h ($P < 0.001$, Steel-Dwass test [Fig. 4F]). These results demonstrated that diaphorin inhibits the overall growth and division of *B. subtilis* cells.

Electron microscopy showed *B. subtilis* damaged by diaphorin. To assess the ultrastructure of *B. subtilis* treated with diaphorin, TEM was performed using *B. subtilis* cultured for 12 h in media with and without 5 mM diaphorin (Fig. 5). Whereas the cell envelope of control *B. subtilis* was smooth (Fig. 5A to D), the surface of cell envelopes of *B. subtilis* treated with 5 mM diaphorin was invariably rough and appeared severely damaged (Fig. 5E to J), suggesting harmful effects of diaphorin on the cell envelope of *B. subtilis*. Additionally, "mesosome"-like structures were frequently observed in *B. subtilis* cells treated with diaphorin (Fig. 5E and F). In some extreme cases, cells were filled with membranous structures similar to mesosomes (Fig. 5I and J). These membranous structures were not conspicuous in control *B. subtilis* (Fig. 5A to D). Mesosomes, which are intracytoplasmic membrane inclusions or invaginations of the plasma membrane, are recognized to be structural artifacts induced by chemical fixatives used to prepare electron microscopic specimens (34). However, such structures are often preferentially observed in bacteria treated with antibacterial agents, including antibiotics and antimicrobial peptides (35–37), indicative of alterations in the cytoplasmic membranes caused by these agents. In this study, high levels of extent and frequency of mesosome-like membranous structures were observed only in diaphorin-treated *B. subtilis*, implying that these ultrastructures reflect the actual effects of diaphorin on *B. subtilis*.

DISCUSSION

The present study revealed that the physiological concentration of diaphorin, a polyketide synthesized by an obligate symbiont of psyllids, inhibits the growth and cell division of *B. subtilis* (a Gram-positive bacterium) but promotes the growth and metabolic activity of

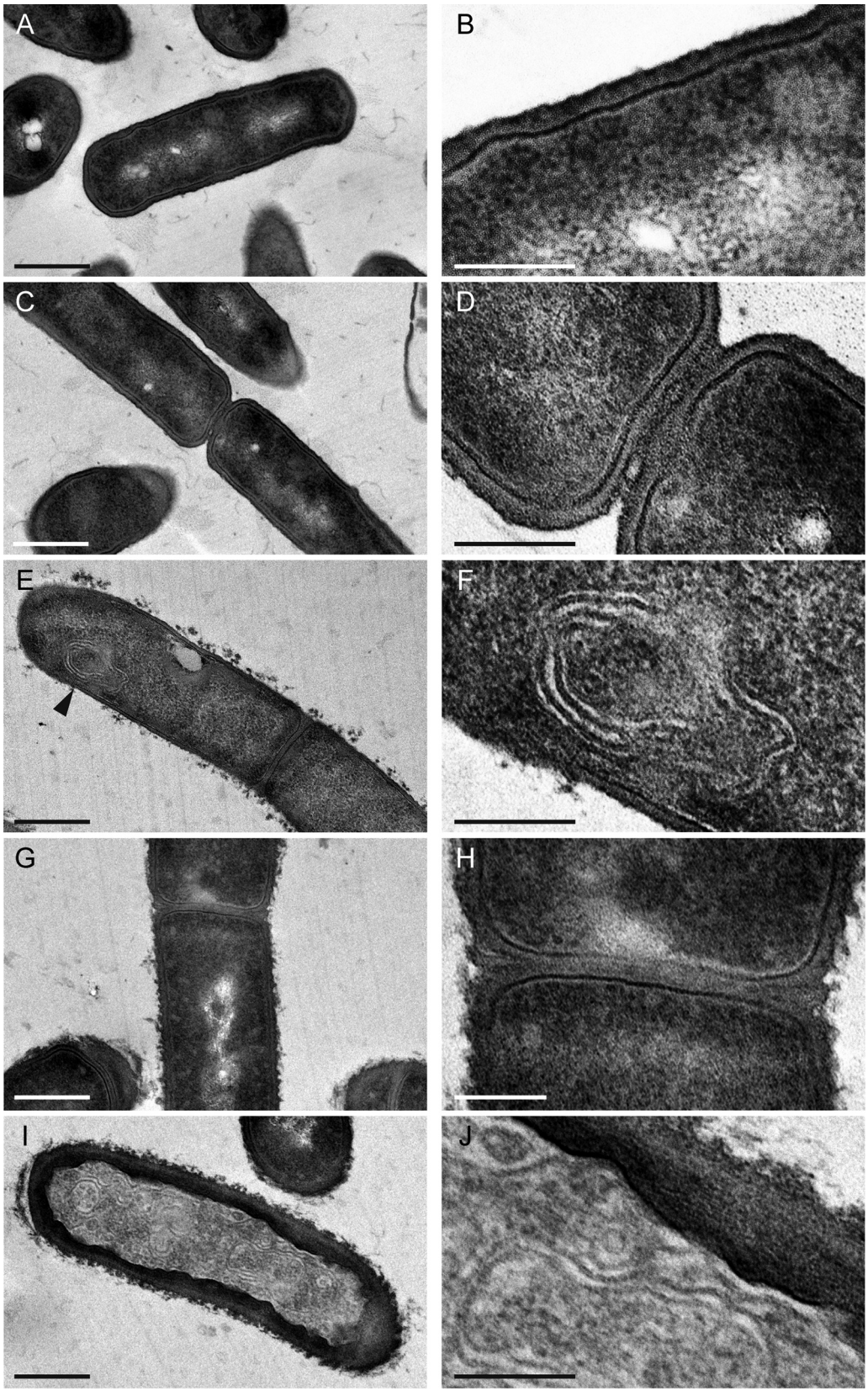

FIG 5 TEM of *B. subtilis* cultured for 12 h in a medium containing 0 mM (A to D) or 5 mM (E to J) diaphorin. Panels B, D, F, H, and J (bars, 200 nm) are magnified images of panels A, C, E, G, and I (bars, 500 nm), respectively. Whereas the cell envelope of control *B. subtilis* was smooth (A to D), the surface of cell envelopes of *B. subtilis* treated with

(Continued on next page)

E. coli (a Gram-negative bacterium). As exemplified by some antibiotics, certain secondary metabolites have inhibitory effects only on Gram-positive bacteria that lack the outer membrane, an effective barrier that protects Gram-negative bacteria from exogenous compounds (2, 4). However, it is unique that a single molecule clearly exhibits opposite effects on distinct bacterial lineages. Particularly, the observed positive effects of diaphorin on *E. coli* attract our interest. As mentioned above, *D. citri* has two bacteriome-associated obligate mutualists, "*Ca*. Carsonella ruddii" (*Gammaproteobacteria*: *Oceanospirillales*), and "*Ca*. Profftella armatura" (*Gammaproteobacteria*: *Burkholderiales*) (21, 22). Additionally, many populations of *D. citri* are infected with *Wolbachia* (*Alphaproteobacteria*: *Rickettsiales*) (12, 31, 38, 39), a potential manipulator of host reproduction, which can be beneficial for certain host lineages (40, 41). Moreover, some *D. citri* populations are infected with "*Ca*. Liberibacter spp." (*Alphaproteobacteria*: *Rhizobiales*), the causative agents of the citrus greening disease, or HLB (9–12, 39). Although *Ca. Liberibacter* was shown to reduce the nymphal development rate and adult survival, it was demonstrated to increase the fecundity, female attractiveness to males, and propensity for dispersal of *D. citri* (42, 43). Thus, this bacterial lineage can also be beneficial for psyllid vectors in some ecological contexts. As with cases in other hemipteran insects (44–57), recent studies are revealing that not only interactions between host psyllids and symbiotic microbes, including those associated with the bacteriome, facultative symbionts, and plant pathogens (19–23, 29), but also interactions among such bacterial populations are important for psyllid biology and host plant pathology (11, 12, 22, 31, 58, 59). Interestingly, all the above-mentioned symbionts in *D. citri*, namely, "*Ca*. Carsonella," "*Ca*. Profftella," *Wolbachia*, and "*Ca*. Liberibacter," belong to the phylum *Proteobacteria* and are closely related to *E. coli*, on which diaphorin exhibited positive effects. The bacteriome-associated obligate mutualists "*Ca*. Carsonella" and "*Ca*. Profftella" are especially close relatives of *E. coli*; all belong to the class *Gammaproteobacteria*. Thus, it would not be farfetched to assume that diaphorin may potentially have positive effects also on these bacterial symbionts, eliminating certain other lineages of bacterial intruders on the other hand. Moreover, in the present study, the results of the β-galactosidase assay indicated that diaphorin remarkably increases the metabolic activity of *E. coli* per culture volume. As *E. coli* is utilized for producing various industrially important materials, including pharmaceutical drugs, amino acids, enzymes, and biofuels (60–63), the observed effects of diaphorin may be exploited to promote the efficiency of industrial material production by *E. coli*.

Regarding the inhibitory effects, although pederin congeners have been shown to inhibit protein synthesis by binding to the E-site of the 60S subunit of eukaryotic ribosomes, little is known about their effects on bacteria and bacterial ribosomes (64, 65). In this study, the long chain of *B. subtilis* was observed at 12 h of incubation with diaphorin, which was reminiscent of the chained cell forms in the biofilm induced by stressors, including antibiotics (66, 67). However, *B. subtilis* failed to form a biofilm at 24 h of incubation, which may reflect the damage to *B. subtilis* caused by diaphorin, as shown by TEM. It is currently uncertain why the chained form was temporally constructed and subsequently resolved and whether interactions between diaphorin and bacterial ribosomes are involved in the overall negative effects observed in this study. Further studies are warranted to elucidate the target microbial spectrum in greater detail and elaborate on the mechanisms underlying both the positive and negative biological activities of diaphorin in bacteria.

Also, in pest management, the target spectrum of diaphorin potentially affects the effectiveness of the biological control of *D. citri* using entomopathogenic bacteria. A notable report on *D. citri* exposed to bacteria (68) showed that Gram-negative bacteria, including *E. coli*, significantly increased the mortality of *D. citri*, but Gram-positive bacteria, including *B. subtilis*, did not. During the experiment, *E. coli* titers increased rapidly after exposure and

FIG 5 Legend (Continued)
diaphorin was invariably rough and appeared disrupted (E to J), suggesting harmful effects of diaphorin on the *B. subtilis* cell envelope. Mesosome-like structures were observed in *B. subtilis* cells treated with diaphorin (E [arrowhead] and F). In some cases, cells were filled with cytoplasmic membranous structures similar to mesosomes (I and J).

remained high until the death of *D. citri* (68), which appeared consistent with the fact that *D. citri* lacks genes for the Imd pathway (69), an immune pathway targeting Gram-negative bacteria with diaminopimelic acid (DAP)-type peptidoglycan (70). In contrast, *D. citri* has a nearly complete Toll immune pathway targeting Gram-positive bacteria with lysine-type peptidoglycan (69). However, *B. subtilis*, the model Gram-positive bacterium, has DAP-type peptidoglycan in its cell wall, like Gram-negative bacteria, and is exclusively recognized by the Imd pathway (71). Thus, it was an enigma why exposure to *B. subtilis* caused no damage to *D. citri*, which lacks the Imd pathway and most genes for antimicrobial peptides (68). The inhibitory effects of diaphorin on *B. subtilis*, demonstrated in the present study, appear to provide the answer to this enigma.

Conclusion. The present study revealed that diaphorin (i) inhibits the growth and cell cleavage of *B. subtilis* and (ii) promotes the growth and metabolic activity of *E. coli*. These findings provide insights into the potential role of diaphorin in facilitating symbiotic associations, manipulating bacterial populations within *D. citri*. This can also be exploited to promote the effectiveness of industrial material production by microorganisms. Further studies are required to reveal the biological activities of diaphorin on more diverse bacterial lineages and the molecular mechanisms for exerting observed activities.

MATERIALS AND METHODS

Preparation of diaphorin. Diaphorin was extracted and purified as described previously (21, 25). Adult *D. citri* insects were ground in methanol, and the extracts were concentrated *in vacuo*. The residue was purified in a Shimadzu (Kyoto, Japan) LC10 high-performance liquid chromatography (HPLC) system with an Inertsil ODS-3 C_{18} reverse-phase preparative column (GL Science, Tokyo, Japan). The purified samples were combined, dried, redissolved in methanol, and filter sterilized using a Minisart syringe filter with a pore size of 0.2 μm (Sartorius, Göttingen, Germany). Aliquots of the purified samples were quantified in the LC10 HPLC system using an Inertsil ODS-3 analytical column (GL Science). The purified diaphorin was stored at −20°C until use.

Transformation of *E. coli*. To confer ampicillin resistance and β-galactosidase activity, *E. coli* strain JM109 was transformed with the pGEM-T Easy vector (Promega, Madison, WI), which encodes β-lactamase and the β-galactosidase α-peptide (LacZα). Cultivation with ampicillin was performed to avoid contamination with other bacteria, and β-galactosidase was introduced for the purpose of the β-galactosidase assay (see below). After self-ligation with T4 DNA ligase at 25°C for 1 h, the vector was introduced into *E. coli* according to the manufacturer's instructions. The nucleotide sequence of *lacZ*α was checked following colony PCR using primers *lacZ*_F (5′-GCGCTGGCAAGTGTAGCGG-3′) and *lacZ*_R (5′-TCCGGCTCGTATGTT GTGTGG-3′), which, respectively, target the 5′ and 3′ flanking regions of the gene. Clones with intact *lacZ*α lacking insertions due to T overhangs were selected and used for the following assays.

Evaluation of the effects of diaphorin on *E. coli*. *E. coli* cells transformed with the pGEM-T Easy plasmid were precultured in Luria-Bertani (LB) medium (1% Bacto tryptone, 0.5% Bacto yeast extract, and 1% NaCl [pH 7.0]) containing 100 μg/mL of ampicillin at 37°C for 14 h with reciprocal shaking (130 rpm). Growth was monitored by measuring the optical density of cultures at 600 nm (OD_{600}) with a NanoDrop 2000c spectrophotometer (Thermo Fisher Scientific, Waltham, MA), with a 1-mm path length. Various diaphorin concentrations (5 μM to 5 mM) were prepared in LB medium containing 100 μg/mL of ampicillin, considering that diaphorin is present in *D. citri* at a concentration of 2 to 20 mM (29) and that some eukaryotes were susceptible to micromolar levels of diaphorin (25). Precultured *E. coli* cells were inoculated into the diaphorin-containing medium, with dilution of the preculture at 1:1,000, and cultured for 24 h as before. The cell density of each culture was analyzed by measuring the OD_{600} as described above. Growth analyses were accompanied by controls cultured in the absence of diaphorin. Four temporally independent experiments were performed, each consisting of three independent cultures in three independent tubes per treatment, giving 12 independent cultures ($n = 12$) per treatment. To assess the direct effects of diaphorin on the optical densities of culture media, time course analyses of OD_{600} of sterile (no inoculation of *E. coli*) medium containing 5 mM diaphorin were also performed at 37°C ($n = 3$).

Transformation of *B. subtilis*. To confer tetracycline resistance, *B. subtilis* strain ISW1214 was transformed with the pHY300PLK (TaKaRa, Kusatsu, Japan) plasmid, which encodes a tetracycline resistance gene. As in the case of *E. coli*, cultivation with tetracycline was carried out to avoid contamination with other bacteria. Transformation of competent *B. subtilis* cells was performed using plasmids preamplified in *E. coli* strain BL21(DE3) according to the manufacturer's instructions.

Evaluation of the effects of diaphorin on *B. subtilis*. *B. subtilis* cells transformed with the pHY300PLK plasmid were precultured in L broth (1% Bacto tryptone, 0.5% Bacto yeast extract, and 0.05% NaCl [pH 7.0]) containing 20 μg/mL of tetracycline at 37°C for 14 h with reciprocal shaking (130 rpm). Growth was monitored by measuring the OD_{600} as described above. Various diaphorin concentrations (5 μM to 5 mM) were prepared in L broth containing 20 μg/mL of tetracycline. Precultured *B. subtilis* cells were inoculated to the diaphorin-containing medium, with dilution of the preculture at 1:1,000, and cultured for 24 h as before. The cell density of each culture was analyzed by measuring the OD_{600}. Growth analyses were accompanied by controls cultured in the absence of diaphorin. Four temporally independent

experiments were performed, each consisting of three independent cultures in three independent tubes per treatment, giving 12 independent cultures ($n = 12$) per treatment. To assess the direct effects of diaphorin on optical densities of culture media, time course analyses of OD_{600} of sterile (no inoculation of *B. subtilis*) medium containing 5 mM diaphorin were also performed at 37°C ($n = 3$).

Assessment of culture purity by amplicon sequencing. To assess the possibility of contamination, bacterial populations in culture media were analyzed using high-throughput amplicon sequencing of the 16S rRNA gene. After cultivation of *E. coli* or *B. subtilis* with or without treatment of 5 mM diaphorin for 24 h, cells were harvested by centrifugation at 16,000 $\times$ *g* for 5 min. Cell pellets were resuspended in suspension buffer, which was transferred into NucleoSpin bead tubes (type B) containing 40- to 400-μm glass beads (Macherey-Nagel, Düren, Germany). The bead tubes were attached to a Vortex-Genie 2 mixer (Scientific Industries, Bohemia, NY) using an MN bead tube holder, and cells were disrupted by agitation at 3,200 rpm for 20 min. Subsequently, DNA was extracted using NucleoSpin microbial DNA columns according to the manufacturer's instructions. Amplicon PCR was performed using extracted DNA, KAPA HiFi HotStart ReadyMix (KAPA Biosystems, Wilmington, MA), and the primer set 16S_341F (5′-TCGTCGGCAGCGTCAGATGTGTATAAGAGACAGCCTACGGGNGGCWGCAG-3′) and 16S_805R (5′-GTCTCGTGGGCTCGGAGATGTGTATAAGAGACAGGACTACHVGGGTATCTAATCC-3′) targeting the V3 and V4 regions of the 16S rRNA gene, based on the instructions by Illumina (San Diego, CA) (72). Dual indices and Illumina sequencing adapters were attached to the amplicons by index PCR using the Nextera XT index kit v2 (Illumina). The libraries were combined with PhiX control v3 (Illumina), and 300 bp of each end was sequenced on the MiSeq platform (Illumina) with the MiSeq reagent kit v3 (600 cycles; Illumina). After the amplicon sequence reads were demultiplexed, the output sequences were imported into the QIIME2 platform (v2020.2) (73) and processed as described previously (31, 58). Obtained sequence variants were manually checked by performing BLASTN searches against the National Center for Biotechnology Information nonredundant database (74).

Optical microscopic analysis. Aliquots of bacterial cultures were put on glass slides, stained with NucBlue Live ReadyProbes reagent (Hoechst 33342 dye; Thermo Fisher Scientific) as needed, and examined by differential interference contrast (DIC) microscopy and/or fluorescence microscopy using a BX53 biological microscope (Olympus, Tokyo, Japan). The morphology of bacterial cells was analyzed using the Fiji package of ImageJ (75). The cell length (major axis) and cell width (minor axis) were measured using the segmented line tool implemented in ImageJ. In this study, even when septa or septum-like structures were observed, a sequential unit was defined as a single cell if it was not cleaved. Cell volume was calculated assuming that cells consist of a cylinder and two half-spheres:

$$V = \pi\left(\frac{w}{2}\right)^2(l - w) + \frac{4}{3}\pi\left(\frac{w}{2}\right)^3 = \frac{\pi w^2}{4}\left(l - \frac{w}{3}\right)$$

where l is cell length and *w* is cell width.

Aliquots of bacterial culture were put into a bacterial counter (depth of 20 μm; Sunlead Glass, Koshigaya, Japan), and cell numbers were counted under a BX53 microscope.

Electron microscopic analysis. Cultured *E. coli* and *B. subtilis* were fixed with 4% paraformaldehyde and 1% glutaraldehyde at 4°C overnight. The fixed samples were washed with phosphate-buffered saline (PBS) and postfixed with 1% osmium tetroxide for 1 h at room temperature. After a washing with PBS, the specimens were dehydrated in a graded ethanol series at room temperature. The samples were treated with propylene oxide and infiltrated with a propylene oxide-Epon (Epon 812 resin; TAAB Laboratories, Aldermaston, UK) solution (propylene oxide-Epon resin, 1:1 [vol/vol]) overnight. The samples were embedded in Epon resin, which was allowed to polymerize at 70°C for 72 h. Ultrathin sections were cut on an ultramicrotome (Leica Reichert Division, Vienna, Austria) and mounted on nickel grids. The sections were stained with 4% uranyl acetate and lead citrate. After staining, all sections were examined under a transmission electron microscope (model JEM1010; JEOL, Tokyo, Japan) operated at 80 kV.

***β*-galactosidase assay.** The β-galactosidase assay was performed according to the method described by Miller (33). *E. coli* cells transformed with the pGEM-T Easy plasmid were precultured in LB medium containing 100 μg/mL of ampicillin at 37°C for 14 h with reciprocal shaking (130 rpm). Precultured *E. coli* cells were inoculated to medium with or without 5 mM diaphorin, with dilution of the preculture at 1:1,000, and cultured as described above. After cultivation for 4 h, isopropyl β-D-1-thiogalactopyranoside (IPTG) was added at a final concentration of 1 mM to induce β-galactosidase synthesis. Three hours after the addition of IPTG, the OD_{600} of each specimen was measured. Subsequently, 10 μL of each culture was transferred to a fresh tube and mixed with 90 μL of Z buffer (60 mM Na_2HPO_4, 40 mM NaH_2PO_4, 10 mM KCl, 1 mM $MgSO_4$, and 50 mM β-mercaptoethanol), 10 μL of chloroform, and 5 μL of 0.1% sodium dodecyl sulfate solution. The tubes were vortexed and left for 1 min at room temperature to permeabilize cells. Subsequently, 20 μL of 4-mg/mL *o*-nitrophenyl-β-D-galactopyranoside was added to each tube. When a yellow color due to *o*-nitrophenyl developed, the reaction was stopped by adding 30 μL of 1 M Na_2CO_3. After centrifugation at 3,000 $\times$ *g* for 1 min, the aqueous phase was removed and used for the OD_{420} and OD_{550} measurements. The β-galactosidase activity was calculated using the following equations:

$$\text{Miller units} = 1{,}000 \times \frac{OD_{420} - 1.75 \times OD_{550}}{t \times v \times OD_{600}} \text{ and } 1{,}000 \times \frac{OD_{420} - 1.75 \times OD_{550}}{t \times v}$$

where *t* is time of the enzymatic reaction (minutes) and *v* is volume of culture used in the assay (milliliters).

Statistical analysis. All statistical analyses were performed using R v4.1.3 (76). Values for bacterial cell sizes were converted into logarithms. The normal distribution of the data was assessed using the Kolmogorov-Smirnov test (77) and the Shapiro-Wilk test (78). When the normal distribution was not rejected, data from two groups were compared using Welch's *t* test (79). When the normal distribution was rejected, data from two groups were compared using the Brunner-Munzel test, a nonparametric method that does not assume homoscedasticity (80). For multiple comparisons, the homogeneity of variances was assessed with the Bartlett test (81). When normal distribution and homogeneous variance of data were not rejected, multiple comparisons were performed using one- or two-way analysis of variance (ANOVA), followed by Dunnett's test (82) or Tukey's test (83). When these null hypotheses were rejected, multiple comparisons were performed using the Kruskal-Wallis test (84), followed by the Steel test (85) or the Steel-Dwass test (86).

Data availability. The nucleotide sequence data are available in the DDBJ/EMBL/GenBank databases under accession numbers DRR355813 to DRR355816.

SUPPLEMENTAL MATERIAL

Supplemental material is available online only.

SUPPLEMENTAL FILE 1, PDF file, 2.9 MB.

SUPPLEMENTAL FILE 2, XLSX file, 0.01 MB.

SUPPLEMENTAL FILE 3, XLSX file, 0.01 MB.

SUPPLEMENTAL FILE 4, XLSX file, 0.01 MB.

SUPPLEMENTAL FILE 5, XLSX file, 0.01 MB.

ACKNOWLEDGMENTS

This work was supported by the Japan Society for the Promotion of Science (https://www.jsps.go.jp) KAKENHI (grant numbers 26292174 and 20H02998), the NIBB Collaborative Research Program for Integrative Imaging (21-417), and research grants from Tatematsu Foundation and Nagase Science and Technology Foundation to A.N. The funders had no role in study design, data collection and analysis, decision to publish, or preparation of the manuscript.

REFERENCES

1. Crits-Christoph A, Diamond S, Butterfield CN, Thomas BC, Banfield JF. 2018. Novel soil bacteria possess diverse genes for secondary metabolite biosynthesis. Nature 558:440–444. https://doi.org/10.1038/s41586-018-0207-y.
2. Lewis K. 2020. The science of antibiotic discovery. Cell 181:29–45. https://doi.org/10.1016/j.cell.2020.02.056.
3. Nayfach S, Roux S, Seshadri R, Udwary D, Varghese N, Schulz F, Wu D, Paez-Espino D, Chen IM, Huntemann M, Palaniappan K, Ladau J, Mukherjee S, Reddy TBK, Nielsen T, Kirton E, Faria JP, Edirisinghe JN, Henry CS, Jungbluth SP, Chivian D, Dehal P, Wood-Charlson EM, Arkin AP, Tringe SG, Visel A, Abreu H, Acinas SG, Allen E, Allen MA, Alteio LV, Andersen G, Anesio AM, Attwood G, Avila-Magaña V, Badis Y, Bailey J, Baker B, Baldrian P, Barton HA, Beck DAC, Becraft ED, Beller HR, Beman JM, Bernier-Latmani R, Berry TD, Bertagnolli A, Bertilsson S, Bhatnagar JM, Bird JT, IMG/M Data Consortium, et al. 2021. A genomic catalog of Earth's microbiomes. Nat Biotechnol 39:499–509. https://doi.org/10.1038/s41587-020-0718-6.
4. Spagnolo F, Trujillo M, Dennehy JJ. 2021. Why do antibiotics exist? mBio 12:e01966-21. https://doi.org/10.1128/mBio.01966-21.
5. Piel J. 2011. Approaches to capturing and designing biologically active small molecules produced by uncultured microbes. Annu Rev Microbiol 65:431–453. https://doi.org/10.1146/annurev-micro-090110-102805.
6. Flórez L, Biedermann PHW, Engl T, Kaltenpoth M. 2015. Defensive symbioses of animals with prokaryotic and eukaryotic microorganisms. Nat Prod Rep 32:904–936. https://doi.org/10.1039/c5np00010f.
7. Adnani N, Rajski SR, Bugni TS. 2017. Symbiosis-inspired approaches to antibiotic discovery. Nat Prod Rep 34:784–814. https://doi.org/10.1039/c7np00009j.
8. Hemmerling F, Piel J. 2022. Strategies to access biosynthetic novelty in bacterial genomes for drug discovery. Nat Rev Drug Discov 21:359–378. https://doi.org/10.1038/s41573-022-00414-6.
9. Grafton-Cardwell EE, Stelinski LL, Stansly PA. 2013. Biology and management of Asian citrus psyllid, vector of the huanglongbing pathogens. Annu Rev Entomol 58:413–432. https://doi.org/10.1146/annurev-ento-120811-153542.
10. Wang N, Pierson EA, Setubal JC, Xu J, Levy JG, Zhang Y, Li J, Rangel LT, Martins J. 2017. The *Candidatus* Liberibacter-host interface: insights into pathogenesis mechanisms and disease control. Annu Rev Phytopathol 55:451–482. https://doi.org/10.1146/annurev-phyto-080516-035513.
11. Hu B, Rao MJ, Deng X, Pandey SS, Hendrich C, Ding F, Wang N, Xu Q. 2021. Molecular signatures between citrus and *Candidatus* Liberibacter asiaticus. PLoS Pathog 17:e1010071. https://doi.org/10.1371/journal.ppat.1010071.
12. Killiny N. 2022. Made for each other: vector-pathogen interfaces in the huanglongbing pathosystem. Phytopathology 112:26–43. https://doi.org/10.1094/PHYTO-05-21-0182-FI.
13. Orduño-Cruz N, Guzmán-Franco AW, Rodríguez-Leyva E, Alatorre-Rosas R, González-Hernández H, Mora-Aguilera G. 2015. *In vivo* selection of entomopathogenic fungal isolates for control of *Diaphorina citri* (Hemiptera: Liviidae). Biol Control 90:1–5. https://doi.org/10.1016/j.biocontrol.2015.05.011.
14. Khan AA, Qureshi JA, Afzal M, Stansly PA. 2016. Two-spotted ladybeetle *Adalia bipunctata* L. (Coleoptera: Coccinellidae): a commercially available predator to control Asian citrus psyllid *Diaphorina citri* (Hemiptera: Liviidae). PLoS One 11:e0162843. https://doi.org/10.1371/journal.pone.0162843.
15. Milosavljevic I, Amrich R, Strode V, Hoddle MS. 2018. Modeling the phenology of Asian citrus psyllid (Hemiptera: Liviidae) in urban southern California: effects of environment, habitat, and natural enemies. Environ Entomol 47:233–243. https://doi.org/10.1093/ee/nvx206.
16. Tiwari S, Mann RS, Rogers ME, Stelinski LL. 2011. Insecticide resistance in field populations of Asian citrus psyllid in Florida. Pest Manag Sci 67:1258–1268. https://doi.org/10.1002/ps.2181.
17. Pardo S, Martínez AM, Figueroa JI, Chavarrieta JM, Viñuela E, Rebollar-Alviter Á, Miranda MA, Valle J, Pineda S. 2018. Insecticide resistance of adults and nymphs of Asian citrus psyllid populations from Apatzingán Valley, Mexico. Pest Manag Sci 74:135–140. https://doi.org/10.1002/ps.4669.
18. Chen XD, Neupane S, Gossett H, Pelz-Stelinski KS, Stelinski LL. 2021. Insecticide rotation scheme restores insecticide susceptibility in thiamethoxam-resistant field populations of Asian citrus psyllid, *Diaphorina citri* Kuwayama (Hemiptera: Liviidae), in Florida. Pest Manag Sci 77:464–473. https://doi.org/10.1002/ps.6039.
19. Nakabachi A, Koshikawa S, Miura T, Miyagishima S. 2010. Genome size of *Pachypsylla venusta* (Hemiptera: Psyllidae) and the ploidy of its bacteriocyte, the symbiotic host cell that harbors intracellular mutualistic bacteria

with the smallest cellular genome. Bull Entomol Res 100:27–33. https://doi.org/10.1017/S0007485309006737.
20. Sloan DB, Nakabachi A, Richards S, Qu J, Murali SC, Gibbs RA, Moran NA. 2014. Parallel histories of horizontal gene transfer facilitated extreme reduction of endosymbiont genomes in sap-feeding insects. Mol Biol Evol 31:857–871. https://doi.org/10.1093/molbev/msu004.
21. Nakabachi A, Ueoka R, Oshima K, Teta R, Mangoni A, Gurgui M, Oldham NJ, Van Echten-Deckert G, Okamura K, Yamamoto K, Inoue H, Ohkuma M, Hongoh Y, Miyagishima S, Hattori M, Piel J, Fukatsu T. 2013. Defensive bacteriome symbiont with a drastically reduced genome. Curr Biol 23:1478–1484. https://doi.org/10.1016/j.cub.2013.06.027.
22. Dan H, Ikeda N, Fujikami M, Nakabachi A. 2017. Behavior of bacteriome symbionts during transovarial transmission and development of the Asian citrus psyllid. PLoS One 12:e0189779. https://doi.org/10.1371/journal.pone.0189779.
23. Nakabachi A, Yamashita A, Toh H, Ishikawa H, Dunbar HE, Moran NA, Hattori M. 2006. The 160-kilobase genome of the bacterial endosymbiont *Carsonella*. Science 314:267. https://doi.org/10.1126/science.1134196.
24. Nakabachi A, Moran NA. 2022. Extreme polyploidy of *Carsonella*, an organelle-like bacterium with a drastically reduced genome. Microbiol Spectr 10:e0035022. https://doi.org/10.1128/spectrum.00350-22.
25. Yamada T, Hamada M, Floreancig P, Nakabachi A. 2019. Diaphorin, a polyketide synthesized by an intracellular symbiont of the Asian citrus psyllid, is potentially harmful for biological control agents. PLoS One 14:e0216319. https://doi.org/10.1371/journal.pone.0216319.
26. Kellner RLL, Dettner K. 1996. Differential efficacy of toxic pederin in deterring potential arthropod predators of *Paederus* (Coleoptera: Staphylinidae) offspring. Oecologia 107:293–300. https://doi.org/10.1007/BF00328445.
27. Piel J. 2002. A polyketide synthase-peptide synthetase gene cluster from an uncultured bacterial symbiont of *Paederus* beetles. Proc Natl Acad Sci U S A 99:14002–14007. https://doi.org/10.1073/pnas.222481399.
28. Kellner RLL. 2002. Molecular identification of an endosymbiotic bacterium associated with pederin biosynthesis in *Paederus sabaeus* (Coleoptera: Staphylinidae). Insect Biochem Mol Biol 32:389–395. https://doi.org/10.1016/S0965-1748(01)00115-1.
29. Nakabachi A, Fujikami M. 2019. Concentration and distribution of diaphorin, and expression of diaphorin synthesis genes during Asian citrus psyllid development. J Insect Physiol 118:103931. https://doi.org/10.1016/j.jinsphys.2019.103931.
30. Nakabachi A, Okamura K. 2019. Diaphorin, a polyketide produced by a bacterial symbiont of the Asian citrus psyllid, kills various human cancer cells. PLoS One 14:e0218190. https://doi.org/10.1371/journal.pone.0218190.
31. Nakabachi A, Malenovský I, Gjonov I, Hirose Y. 2020. 16S rRNA sequencing detected *Profftella*, *Liberibacter*, *Wolbachia*, and *Diplorickettsia* from relatives of the Asian citrus psyllid. Microb Ecol 80:410–422. https://doi.org/10.1007/s00248-020-01491-z.
32. Nakabachi A, Piel J, Malenovský I, Hirose Y. 2020. Comparative genomics underlines multiple roles of *Profftella*, an obligate symbiont of psyllids: providing toxins, vitamins, and carotenoids. Genome Biol Evol 12:1975–1987. https://doi.org/10.1093/gbe/evaa175.
33. Miller JH. 1972. Experiments in molecular genetics. Cold Spring Harbor Laboratory Press, Cold Spring Harbor, NY.
34. Pilhofer M, Ladinsky MS, McDowall AW, Jensen GJ. 2010. Bacterial TEM: new insights from cryo-microscopy. Methods Cell Biol 96:21–45. https://doi.org/10.1016/S0091-679X(10)96002-0.
35. Balkwill DL, Stevens SE. 1980. Effects of penicillin G on mesosome-like structures in *Agmenellum quadruplicatum*. Antimicrob Agents Chemother 17:506–509. https://doi.org/10.1128/AAC.17.3.506.
36. De León L, Moujir L. 2008. Activity and mechanism of the action of zeylasterone against *Bacillus subtilis*. J Appl Microbiol 104:1266–1274. https://doi.org/10.1111/j.1365-2672.2007.03663.x.
37. Li Z, Mao R, Teng D, Hao Y, Chen H, Wang X, Wang X, Yang N, Wang J. 2017. Antibacterial and immunomodulatory activities of insect defensins-DLP2 and DLP4 against multidrug-resistant *Staphylococcus aureus*. Sci Rep 7:12124. https://doi.org/10.1038/s41598-017-10839-4.
38. Subandiyah S, Nikoh N, Tsuyumu S, Somowiyarjo S, Fukatsu T. 2000. Complex endosymbiotic microbiota of the citrus psyllid *Diaphorina citri* (Homoptera: Psylloidea). Zool Sci 17:983–989. https://doi.org/10.2108/zsj.17.983.
39. Morrow JL, Om N, Beattie GAC, Chambers GA, Donovan NJ, Liefting LW, Riegler M, Holford P. 2020. Characterization of the bacterial communities of psyllids associated with Rutaceae in Bhutan by high throughput sequencing. BMC Microbiol 20:215. https://doi.org/10.1186/s12866-020-01895-4.
40. Werren JH, Baldo L, Clark ME. 2008. *Wolbachia*: master manipulators of invertebrate biology. Nat Rev Microbiol 6:741–751. https://doi.org/10.1038/nrmicro1969.
41. Pascar J, Chandler CH. 2018. A bioinformatics approach to identifying *Wolbachia* infections in arthropods. PeerJ 6:e5486. https://doi.org/10.7717/peerj.5486.
42. Pelz-Stelinski KS, Killiny N. 2016. Better together: association with '*Candidatus* Liberibacter asiaticus' increases the reproductive fitness of its insect vector, *Diaphorina citri* (Hemiptera: Liviidae). Ann Entomol Soc Am 109:371–376. https://doi.org/10.1093/aesa/saw007.
43. Martini X, Hoffmann M, Coy MR, Stelinski LL, Pelz-Stelinski KS. 2015. Infection of an insect vector with a bacterial plant pathogen increases its propensity for dispersal. PLoS One 10:e0129373. https://doi.org/10.1371/journal.pone.0129373.
44. Nakabachi A, Ishikawa H. 1997. Differential display of mRNAs related to amino acid metabolism in the endosymbiotic system of aphids. Insect Biochem Mol Biol 27:1057–1062. https://doi.org/10.1016/s0965-1748(97)00092-1.
45. Nakabachi A, Ishikawa H. 1999. Provision of riboflavin to the host aphid, *Acyrthosiphon pisum*, by endosymbiotic bacteria, *Buchnera*. J Insect Physiol 45:1–6. https://doi.org/10.1016/S0022-1910(98)00104-8.
46. Nakabachi A, Ishikawa H. 2000. Polyamine composition and expression of genes related to polyamine biosynthesis in an aphid endosymbiont, *Buchnera*. Appl Environ Microbiol 66:3305–3309. https://doi.org/10.1128/AEM.66.8.3305-3309.2000.
47. Nakabachi A, Ishikawa H, Kudo T. 2003. Extraordinary proliferation of microorganisms in aposymbiotic pea aphids, *Acyrthosiphon pisum*. J Invertebr Pathol 82:152–161. https://doi.org/10.1016/s0022-2011(03)00020-x.
48. Nakabachi A, Shigenobu S, Sakazume N, Shiraki T, Hayashizaki Y, Carninci P, Ishikawa H, Kudo T, Fukatsu T. 2005. Transcriptome analysis of the aphid bacteriocyte, the symbiotic host cell that harbors an endocellular mutualistic bacterium, *Buchnera*. Proc Natl Acad Sci U S A 102:5477–5482. https://doi.org/10.1073/pnas.0409034102.
49. Moran NA, McCutcheon JP, Nakabachi A. 2008. Genomics and evolution of heritable bacterial symbionts. Annu Rev Genet 42:165–190. https://doi.org/10.1146/annurev.genet.41.110306.130119.
50. Nikoh N, Nakabachi A. 2009. Aphids acquired symbiotic genes via lateral gene transfer. BMC Biol 7:12. https://doi.org/10.1186/1741-7007-7-12.
51. Gerardo NM, Altincicek B, Anselme C, Atamian H, Barribeau SM, de Vos M, Duncan EJ, Evans JD, Gabaldón T, Ghanim M, Heddi A, Kaloshian I, Latorre A, Moya A, Nakabachi A, Parker BJ, Pérez-Brocal V, Pignatelli M, Rahbé Y, Ramsey JS, Spragg CJ, Tamames J, Tamarit D, Tamborindeguy C, Vincent-Monegat C, Vilcinskas A. 2010. Immunity and other defenses in pea aphids, *Acyrthosiphon pisum*. Genome Biol 11:R21. https://doi.org/10.1186/gb-2010-11-2-r21.
52. Nikoh N, McCutcheon JP, Kudo T, Miyagishima S, Moran NA, Nakabachi A. 2010. Bacterial genes in the aphid genome: absence of functional gene transfer from *Buchnera* to its host. PLoS Genet 6:e1000827. https://doi.org/10.1371/journal.pgen.1000827.
53. Tamborindeguy C, Monsion B, Brault V, Hunnicutt L, Ju HJ, Nakabachi A, Van Fleet E. 2010. A genomic analysis of transcytosis in the pea aphid, *Acyrthosiphon pisum*, a mechanism involved in virus transmission. Insect Mol Biol 19:259–272. https://doi.org/10.1111/j.1365-2583.2009.00956.x.
54. Shigenobu S, Richards S, Cree AGG, Morioka M, Fukatsu T, Kudo T, Miyagishima S, Gibbs RAA, Stern DLL, Nakabachi A. 2010. A full-length cDNA resource for the pea aphid, *Acyrthosiphon pisum*. Insect Mol Biol 19:23–31. https://doi.org/10.1111/j.1365-2583.2009.00946.x.
55. Nakabachi A, Miyagishima S. 2010. Expansion of genes encoding a novel type of dynamin in the genome of the pea aphid, *Acyrthosiphon pisum*. Insect Mol Biol 19:165–173. https://doi.org/10.1111/j.1365-2583.2009.00941.x.
56. Nakabachi A, Ishida K, Hongoh Y, Ohkuma M, Miyagishima S. 2014. Aphid gene of bacterial origin encodes protein transported to obligate endosymbiont. Curr Biol 24:R640–R641. https://doi.org/10.1016/j.cub.2014.06.038.
57. Nakabachi A. 2015. Horizontal gene transfers in insects. Curr Opin Insect Sci 7:24–29. https://doi.org/10.1016/j.cois.2015.03.006.
58. Nakabachi A, Inoue H, Hirose Y. 2022. Microbiome analyses of 12 psyllid species of the family Psyllidae identified various bacteria including *Fukatsuia* and *Serratia symbiotica*, known as secondary symbionts of aphids. BMC Microbiol 22:15. https://doi.org/10.1186/s12866-021-02429-2.
59. Nakabachi A, Nikoh N, Oshima K, Inoue H, Ohkuma M, Hongoh Y, Miyagishima S, Hattori M, Fukatsu T. 2013. Horizontal gene acquisition of *Liberibacter* plant pathogens from a bacteriome-confined endosymbiont of their psyllid vector. PLoS One 8:e82612. https://doi.org/10.1371/journal.pone.0082612.

60. Peralta-Yahya PP, Zhang F, Del Cardayre SB, Keasling JD. 2012. Microbial engineering for the production of advanced biofuels. Nature 488:320–328. https://doi.org/10.1038/nature11478.
61. Rosano GL, Ceccarelli EA. 2014. Recombinant protein expression in *Escherichia coli*: advances and challenges. Front Microbiol 5:172. https://doi.org/10.3389/fmicb.2014.00172.
62. Zhang X, Xu G, Shi J, Koffas MAG, Xu Z. 2018. Microbial production of L-serine from renewable feedstocks. Trends Biotechnol 36:700–712. https://doi.org/10.1016/j.tibtech.2018.02.001.
63. Castro D, Marques ASC, Almeida MR, de Paiva GB, Bento HBS, Pedrolli DB, Freire MG, Tavares APM, Santos-Ebinuma VC. 2021. L-asparaginase production review: bioprocess design and biochemical characteristics. Appl Microbiol Biotechnol 105:4515–4534. https://doi.org/10.1007/s00253-021-11359-y.
64. Tiboni O, Parisi B, Ciferri O. 1968. The mode of action of pederin, a drug inhibiting protein synthesis in eucaryotic organisms. G Bot Ital 102:337–345. https://doi.org/10.1080/11263506809426470.
65. Dmitriev SE, Vladimirov DO, Lashkevich KA. 2020. A quick guide to small-molecule inhibitors of eukaryotic protein synthesis. Biochemistry (Mosc) 85:1389–1421. https://doi.org/10.1134/S0006297920110097.
66. Losick RM. 2020. *Bacillus subtilis*: a bacterium for all seasons. Curr Biol 30:R1146–R1150. https://doi.org/10.1016/j.cub.2020.06.083.
67. Grobas I, Polin M, Asally M. 2021. Swarming bacteria undergo localized dynamic phase transition to form stress-induced biofilms. eLife 10:e62632. https://doi.org/10.7554/eLife.62632.
68. Arp AP, Martini X, Pelz-Stelinski KS. 2017. Innate immune system capabilities of the Asian citrus psyllid, *Diaphorina citri*. J Invertebr Pathol 148:94–101. https://doi.org/10.1016/j.jip.2017.06.002.
69. Arp AP, Hunter WB, Pelz-Stelinski KS. 2016. Annotation of the Asian citrus psyllid genome reveals a reduced innate immune system. Front Physiol 7:570. https://doi.org/10.3389/fphys.2016.00570.
70. Lemaitre B, Kromer-Metzger E, Michaut L, Nicolas E, Meister M, Georgel P, Reichhart JM, Hoffmann JA. 1995. A recessive mutation, immune deficiency (imd), defines two distinct control pathways in the *Drosophila* host defense. Proc Natl Acad Sci U S A 92:9465–9469. https://doi.org/10.1073/pnas.92.21.9465.
71. Takehana A, Yano T, Mita S, Kotani A, Oshima Y, Kurata S. 2004. Peptidoglycan recognition protein (PGRP)-LE and PGRP-LC act synergistically in *Drosophila* immunity. EMBO J 23:4690–4700. https://doi.org/10.1038/sj.emboj.7600466.
72. Illumina. 2013. 16S metagenomic sequencing library preparation part#1504 4223 rev. B. Illumina, San Diego, CA.
73. Bolyen E, Rideout JR, Dillon MR, Bokulich NA, Abnet CC, Al-Ghalith GA, Alexander H, Alm EJ, Arumugam M, Asnicar F, Bai Y, Bisanz JE, Bittinger K, Brejnrod A, Brislawn CJ, Brown CT, Callahan BJ, Caraballo-Rodríguez AM, Chase J, Cope EK, Da Silva R, Diener C, Dorrestein PC, Douglas GM, Durall DM, Duvallet C, Edwardson CF, Ernst M, Estaki M, Fouquier J, Gauglitz JM, Gibbons SM, Gibson DL, Gonzalez A, Gorlick K, Guo J, Hillmann B, Holmes S, Holste H, Huttenhower C, Huttley GA, Janssen S, Jarmusch AK, Jiang L, Kaehler BD, Kang KB, Keefe CR, Keim P, Kelley ST, Knights D, et al. 2019. Reproducible, interactive, scalable and extensible microbiome data science using QIIME 2. Nat Biotechnol 37:852–857. https://doi.org/10.1038/s41587-019-0209-9.
74. Camacho C, Coulouris G, Avagyan V, Ma N, Papadopoulos J, Bealer K, Madden TL. 2009. BLAST+: architecture and applications. BMC Bioinformatics 10:421. https://doi.org/10.1186/1471-2105-10-421.
75. Schindelin J, Arganda-Carreras I, Frise E, Kaynig V, Longair M, Pietzsch T, Preibisch S, Rueden C, Saalfeld S, Schmid B, Tinevez J, White DJ, Hartenstein V, Eliceiri K, Tomancak P, Cardona A. 2012. Fiji: an open-source platform for biological-image analysis. Nat Methods 9:676–682. https://doi.org/10.1038/nmeth.2019.
76. R Core Team. 2021. R: a language and environment for statistical computing. R Foundation for Statistical Computing, Vienna, Austria.
77. Smirnov N. 1948. Table for estimating the goodness of fit of empirical distributions. Ann Math Statist 19:279–281. https://doi.org/10.1214/aoms/1177730256.
78. Shapiro SS, Wilk MB. 1965. An analysis of variance test for normality (complete samples). Biometrika 52:591–611. https://doi.org/10.2307/2333709.
79. Welch BL. 1938. The significance of the difference between two means when the population variances are unequal. Biometrika 29:350–362. https://doi.org/10.2307/2332010.
80. Brunner E, Munzel U. 2000. The nonparametric Behrens-Fisher problem: asymptotic theory and a small-sample approximation. Biom J 42:17–25. https://doi.org/10.1002/(SICI)1521-4036(200001)42:1%3C17::AID-BIMJ17%3E3.0.CO;2-U.
81. Snedecor GW, Cochran WG. 1989. Statistical methods, 8th ed. Iowa State University Press, Ames, IA.
82. Dunnett CW. 1955. A multiple comparison procedure for comparing several treatments with a control. J Am Stat Assoc 50:1096–1121. https://doi.org/10.1080/01621459.1955.10501294.
83. Tukey J. 1949. Comparing individual means in the analysis of variance. Biometrics 5:99–114. https://doi.org/10.2307/3001913.
84. Kruskal WH, Wallis WA. 1952. Use of ranks in one-criterion variance analysis. J Am Stat Assoc 47:583–621. https://doi.org/10.1080/01621459.1952.10483441.
85. Steel RGD. 1959. A multiple comparison rank sum test: treatments versus control. Biometrics 15:560–572. https://doi.org/10.2307/2527654.
86. Steel RGD. 1961. Some rank sum multiple comparisons tests. Biometrics 17:539–552. https://doi.org/10.2307/2527854.